Supporting Information for:

Supplementary Material (ESI) for Chemical Communications

Solvation, substituent effects and cooperativity in edge-to-face aromatic interactions

Scott L. Cockroft* and Christopher A. Hunter*

Dr. Scott L. Cockroft, School of Chemistry, University of Edinburgh, The King's Buildings, West Mains Road, Edinburgh, EH9 3JJ, UK, E-mail: scott.cockroft@ed.ac.uk

Prof. Christopher A. Hunter, Centre for Chemical Biology, Krebs Institute for Biomolecular Science, Department of Chemistry, University of Sheffield, Sheffield, S3 7HF, UK, E-mail: c.hunter@shef.ac.uk

Calculation of α/β H-bond donor/acceptor constants.

Electrostatic surface potentials were calculated at both DFT/B3LYP/6-31G* and AM1 levels using *Spartan '04* (Wavefunction, Irvine).[1] α/β H-bond constants at the positions specified in Figures S3 and S7 were calculated by dividing the calculated electrostatic surface potential (in kJ mol^{-1} at the default isovalue 0.002 electron/Bohr^3) by a factor of 52 kJ mol^{-1} in accordance with the correlations with experimentally determined H-bond constants described in reference 6.

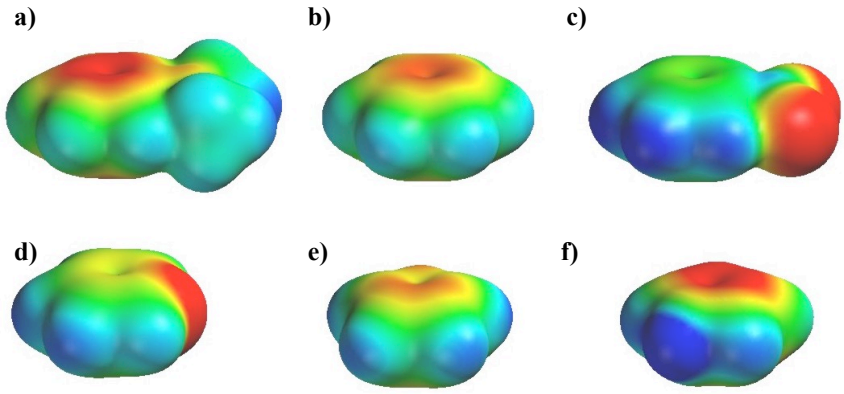

Fig S1. DFT/B3LYP/6-31G* electrostatic potential surfaces (ESPs) of a selection of aromatic rings. a) dimethylaminobenzene, b) benzene, c) nitrobenzene, d) pyridine, f) furan, g) pyrrole. Electrostatic potentials are coloured red to blue (-100 to +100 kJ mol^{-1}), with green representing neutral charge.

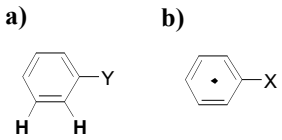

Fig S2. Model compounds used for the calculation of DFT/B3LYP/6-31G* and AM1 electrostatic surface potentials (ESPs) of the edge a), and face b) of the interacting aromatic groups in the molecular torsion balances.

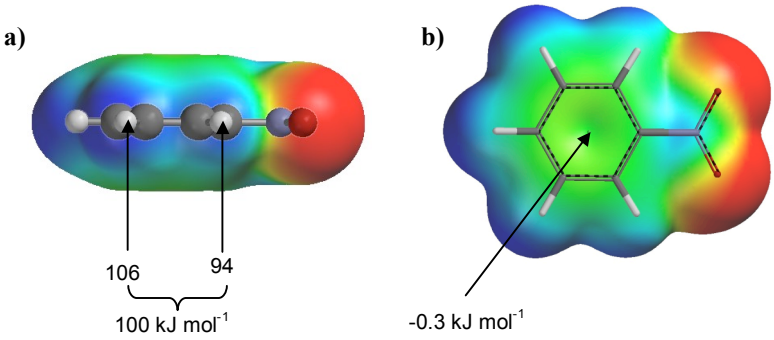

Fig S3. DFT/B3LYP/6-31G* electrostatic surface potentials (ESPs) of the edge a) and face b) of model compounds for molecular torsion balances where X and Y = NO_2. The mean ESP of the two protons on the edge of each aromatic group was taken at the 0.002 electron/Bohr^3 isosurface (viewed in the plane of the aromatic ring and perpendicular to the C-C bond of the ring). The ESPs of aromatic faces were taken at the 0.002 electron/Bohr^3 isosurface in the centre of the aromatic ring of the model compounds.

Table S1. Folding free energies (kJ mol^{-1}) of molecular torsion balances and corresponding β H-bond acceptor constants of the aromatic face as the face substituent X is varied (as plotted in Figure 3 and Figure S4).[8]

		$\Delta\Delta G$			
Y	X	C_6D_6	$CDCl_3$	β_{DFT}	β_{AM1}
CF_3	NH_2	-3.91	-2.65	2.0	2.4
CF_3	H	-3.47	-2.41	1.6	1.9
CF_3	OH	-3.46	-2.32	1.5	1.7
CF_3	I	-1.52	-0.61	1.0	1.5
CF_3	Br	-1.89	-1.01	0.9	1.4
CF_3	NO_2	-0.19	-0.47	0.0	0.1
H	NH_2	-1.95	-0.89	2.0	2.4
H	H	-1.56	-1.00	1.6	1.9
H	OH	-1.61	-1.04	1.5	1.7
H	I	-2.11	-1.37	1.0	1.5
H	Br	-2.01	-1.41	0.9	1.4
H	NO_2	-1.28	-0.96	0.0	0.1

Table S2. Folding free energies of molecular torsion balances and corresponding α H-bond donor constants of the aromatic face as the edge substituent Y is varied in $CDCl_3$ (as plotted in Figures 5 and S5).

Y	X	$\Delta\Delta G$	α_{DFT}	α_{AM1}	Reference
OEt	CH_3	-1.00	0.9	0.7	4
CH_3	CH_3	-1.34	1.0	0.8	4
F	CH_3	-2.13	1.5	1.2	4
Br	CH_3	-2.55	1.6	1.2	4
I	CH_3	-2.64	1.6	1.1	4
NO_2	CH_3	-2.43	1.9	1.7	4
H	CH_3	-1.30	1.1	0.8	3a
OCH_3	CH_3	-0.84	0.9	0.8	2
CH_3	CH_3	-1.38	1.0	0.8	2
CN	CH_3	-2.55	1.9	1.5	2
NO_2	CH_3	-2.55	1.9	1.7	2
I	CH_3	-2.55	1.6	1.1	2
H	H	-1.00	1.1	0.8	5
CF_3	H	-2.31	1.7	1.5	5

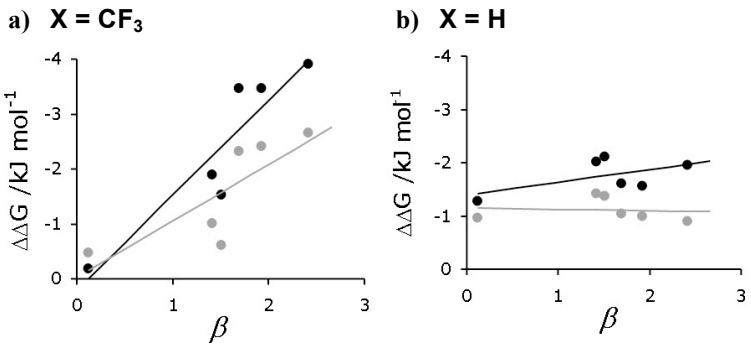

Fig S4. Experimental folding free energies for molecular torsion balances where Y = CF_3 (a) and Y = H (b) in C_6D_6 (black) and $CDCl_3$ (grey) *versus* the H-bond acceptor constants (β) of the aromatic face as the X-substituent is varied (from NO_2 to NH_2). H-bond donor constants were derived from AM1 electrostatic surface potentials (see the main text for the DFT/B3LYP/6-31G* version of this plot).

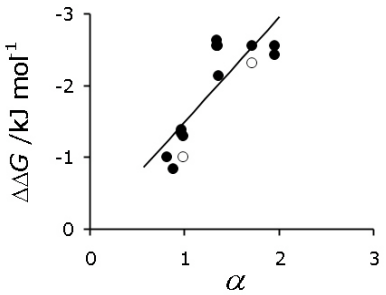

Fig S5. Experimental folding free energies for molecular torsion balances where X = Me (black) and X = H (unfilled circles) in $CDCl_3$ (grey) versus the H-bond donor constants (β) of the aromatic edge protons as the Y-substituent is varied (from OEt to NO_2). H-bond donor constants were derived from AM1 electrostatic surface potentials (see the main text for the DFT/B3LYP/6-31G* version of this plot).

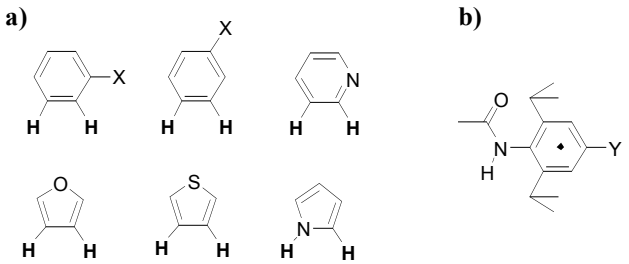

Fig S6. Model compounds used for the calculation of DFT/B3LYP/6-31G* and AM1 electrostatic surface potentials (ESPs) of the edge a), and face b) of the interacting aromatic groups in the zipper complexes in Figure 6.

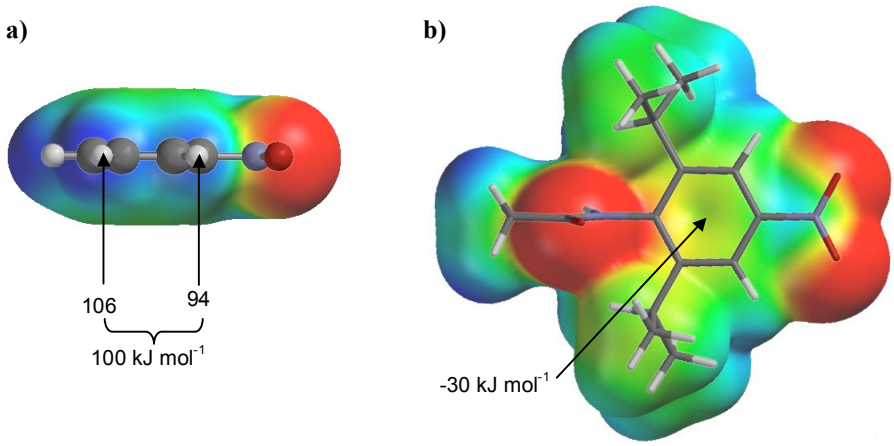

Fig S7. DFT/B3LYP/6-31G* electrostatic surface potentials (ESPs) of the edge a) and face b) of computational models where X and Y = NO_2. The mean ESP of the two protons on the edge of each aromatic group was taken at the 0.002 electron/Bohr^3 isosurface (viewed in the plane of the aromatic ring and perpendicular to the C-C bond of the ring). The ESPs of aromatic faces were taken at the 0.002 electron/Bohr^3 isosurface in the centre of the aromatic ring of the model compounds.

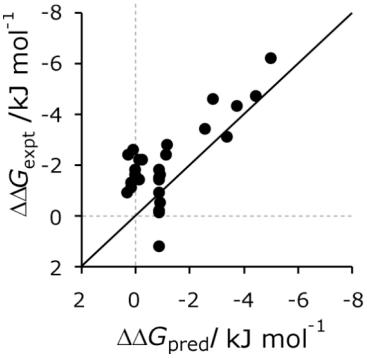

Fig S8. Experimental aromatic interaction energies for edge-to-face aromatic interactions measured in supramolecular zipper complexes in $CDCl_3$ *versus* interaction energies predicted using equation 3 and α/β values derived from AM1 electrostatic surface potentials (see the main text for the DFT/B3LYP/6-31G* version of this plot).

Table S3. Interaction free energies for edge-to-face interactions in $CDCl_3$ (kJ mol^{-1}) determined using chemical double mutant cycles in zipper complexes at 296 ± 2 K. Errors are less than 1 kJ mol^{-1}.

Interaction	Y	X	$\Delta\Delta G_{expt}$	α_{DFT}	α_{AM1}	β_{DFT}	β_{AM1}
	*p*-NMe_2	NMe_2	-0.9	0.9	0.8	2.3	2.6
	p-NMe_2	H	-1.1	0.9	0.8	1.9	2.3
	p-NMe_2	NO_2	-1.4	0.9	0.8	0.6	0.8
	p-tBu	NMe_2	-1.3	1.1	0.8	2.3	2.6
	p-tBu	H	-1.6	1.1	0.8	1.9	2.3
	p-tBu	NO_2	-0.1	1.1	0.8	0.6	0.8
	H	NMe_2	-1.8	1.1	0.9	2.3	2.6
	H	H	-1.4	1.1	0.9	1.9	2.3
	H	NO_2	-0.2	1.1	0.9	0.6	0.8
	p-NO_2	NMe_2	-4.6	1.9	1.7	2.3	2.6
	p-NO_2	H	-3.4	1.9	1.7	1.9	2.3
	p-NO_2	NO_2	+1.2	1.9	1.7	0.6	0.8
	m-NO_2	NMe_2	-4.3	2.1	1.9	2.3	2.6
	m-NO_2	H	-3.1	2.1	1.9	1.9	2.3
	m-NO_2	NO_2	-0.5	2.1	1.9	0.6	0.8
		NMe_2	-2.8	1.4	1.2	2.3	2.6
	-	H	-2.4	1.4	1.2	1.9	2.3
		NO_2	-0.9	1.4	1.2	0.6	0.8
		NMe_2	-2.2	1.3	0.9	2.3	2.6
	-	H	-2.2	1.3	0.9	1.9	2.3
		NO_2	-1.5	1.3	0.9	0.6	0.8
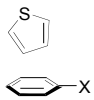		NMe_2	-2.4	1.4	0.8	2.3	2.6
		H	-2.6	1.4	0.8	1.9	2.3
		NO_2	-1.8	1.4	0.8	0.6	0.8
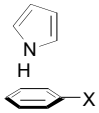		NMe_2	-6.2	2.8	2.3	2.3	2.6
		H	-4.7	2.8	2.3	1.9	2.3
		NO_2	-1.6	2.8	2.3	0.6	0.8

Supporting references

1. J. Kong, C. A. White, A. I. Krylov, D. Sherrill, R. D. Adamson, T. R. Furlani, M. S. Lee, A. M. Lee, S. R. Gwaltney, T. R. Adams, C. Ochsenfeld, A. T. B. Gilbert, G. S. Kedziora, V. A. Rassolov, D. R. Maurice, N. Nair, Y. Shao, N. A. Besley, P. E. Maslen, J. P. Dombroski, H. Daschel, W. Zhang, P. P. Korambath, J. Baker, E. F. C. Byrd, T. Van Voorhis, M. Oumi, S. Hirata, C.-P. Hsu, N. Ishikawa, J. Florian, A. Warshel, B. G. Johnson, P. M. W. Gill, M. Head-Gordon, and J. A. Pople, *J. Comp. Chem.* **21**, 1532-1548 (2000).